Diamond & Related Materials 18 (2009) 957–962

Contents lists available at ScienceDirect

Diamond & Related Materials

journal homepage: www.elsevier.com/locate/diamond

Use of carbon nanotubes for VLSI interconnects

J. Robertson [a,*], G. Zhong [a], S. Hofmann [a], B.C. Bayer [a], C.S. Esconjauregui [a], H. Telg [b], C. Thomsen [b]

[a] Engineering Department, University of Cambridge, Cambridge CB2 1PZ, UK
[b] Department of Physics, Technical University of Berlin, Hardenbergstrasse, Berlin, D-10623 Germany

ARTICLE INFO

Available online 13 February 2009

Keywords:
Carbon nanotubes
Electronic applications
Chemical vapour deposition
Growth

ABSTRACT

The requirements for using carbon nanotubes as interconnects in future integrated circuits are defined. Growth techniques and some methods of their characterisation are described. The need to grow nanotubes on conducting metal substrates is pointed out and this effort is starting.

1. Introduction

The continued scaling of semiconductor devices in VLSI integrated circuits means that there is a replacement of many of the traditional materials used. Copper has replaced aluminium in interconnects, low dielectric constant materials have replaced SiO_2 as the inter-metal dielectric, while high dielectric constant oxides like HfO_2 have replaced SiO_2 as the gate oxide.

Interconnects are the metal wires which pass current between the transistors and are oriented both vertically and horizontally, see Fig. 1. There is a need at the 22 nm node and beyond to consider replacing Cu as the interconnect. This is for two reasons. First, the current density carried by the interconnects will exceed the maximum current density of 6×10^6 A/cm^2 that copper can carry before it could fail due to electromigration [1], Fig. 2. Carbon nanotubes (CNTs) are the only material (except graphene) which can carry a much higher current density, being able to carry up to ~10^9 A/cm^2 before failure [2,3]. This is clear from the initial current vs. voltage plot found by the Yao et al [2], Fig. 3.

The second reason is time delays in the integrated circuit. As dimensions have shrunk, the time delay is no longer dominated by the switching time constant of the transistor but to the RC time constant of the interconnect, due to the interconnect resistance R and its capacitance to the surroundings C (Fig. 4). Long nanotubes can have lower resistances, which cuts down the RC time constant for long interconnects [1].

A third reason for possibly using nanotubes is the aspect ratio. It is difficult to make copper interconnects which have a large aspect ratio (height/length) for putting into deep vertical holes [4]. Here, the interconnect (or Via) is not limited by its current density or resistance, just by its manufacturability.

Despite these three advantages of carbon nanotubes, their use as interconnects is not trivial, because of quantum effects. The resistance of a nanotube-based interconnect must be comparable or lower than that of the copper equivalent. Now, the resistivity of a copper wire increases as its diameter gets smaller, because of side-wall scattering, as shown in Fig. 5. This is equivalent to the copper wire becoming more like a one-dimensional conductor, bulk scattering continues, but side-wall scattering increases as a proportion.

The conductivity of a one-dimensional conductor like a carbon nanotube is limited by one quantum of conductance G_0/conducting channel. For nanotubes, there are two conducting channels/wall of the nanotube. The factor two arises because in the band structure of any metallic nanotube wall, there are two bands that cross the Fermi level.

The quantum of conductance appears as a series resistance in the overall equivalent circuit. Nanotubes are well known for having a ballistic conductance, which enhances their conductance at moderate lengths, but the quantum conductance limits their resistance at short lengths. Thus, the overall resistance of a nanotube interconnect is given by

$$R = \left(R_q + rL\right) / 2n$$

where R_q is the quantum of conductance, $R_q = 12.6$ kΩ/channel, r is the incremental resistivity/unit length of the nanotube, L is its length, and n is the number of walls in the interconnect (Fig. 6). Clearly, in order to minimise the resistance of the interconnect and make it less than the Cu equivalent, the objective is to maximise the number of walls in the interconnect space.

There are two possibilities for nanotube interconnects to maximise n, use one or more multi-walled nanotubes (MWNTs) or use a very high density of single walled nanotubes (SWNTs). MWNTs are always metallic because they always have one wall which is metallic. However, the problem with MWNTs is that only the outer wall tends to carry current, unless the inner walls are properly contacted, and current is forced down them. On the other hand, SWNTs can be either semiconducting or metallic, and it is essential that the fraction of metallic SWNTs is maximised.

The conductance of nanotubes is complex, because it is non-linear, Fig. 3. At low voltages, carrier scattering in CNTs is low, and resistance is low. Then, above a voltage of ~0.2 V, the scattering increases

* Corresponding author.
E-mail address: jr214@hermes.cam.ac.uk (J. Robertson).

0925-9635/$ – see front matter © 2009 Elsevier B.V. All rights reserved.
doi:10.1016/j.diamond.2009.02.008

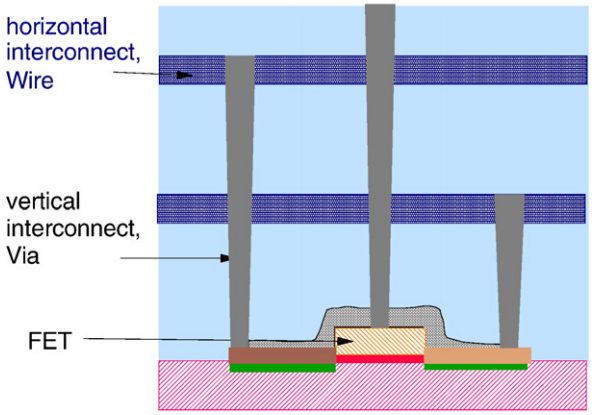

Fig. 1. Schematic of vertical and horizontal interconnects in an integrated circuit.

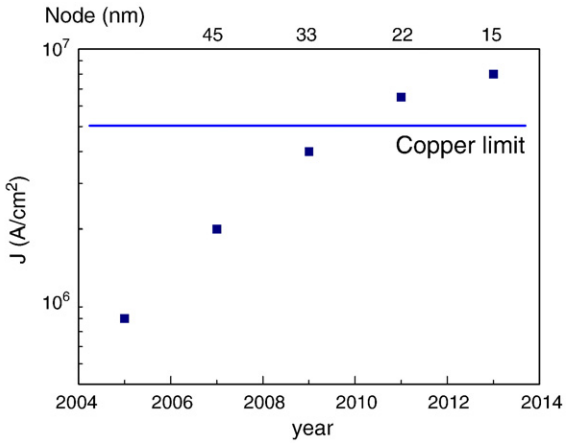

Fig. 2. Current density as a function of year and technology node in the ITRS roadmap.

markedly, as now carriers can be scattered by optical phonons, particularly the zone boundary phonons equivalent to the graphite *K* point, as realised by Yao et al [2]. The resistance vs voltage has been evaluated by Park et al [5], which allows us to extract a resistance/unit length (r) outside the ballistic regime, for both the low field and high field regimes. Note that interconnects will be operating for supply voltages of 0.5 V or under, so that they must be operating in the low voltage regime, or there is a fault.

Overall, the wall density in the interconnect diameter must be maximised. For MWNTs, their typical geometry tends to have a sizable inner tube radius, so that much of their cross sectional area is wasted.

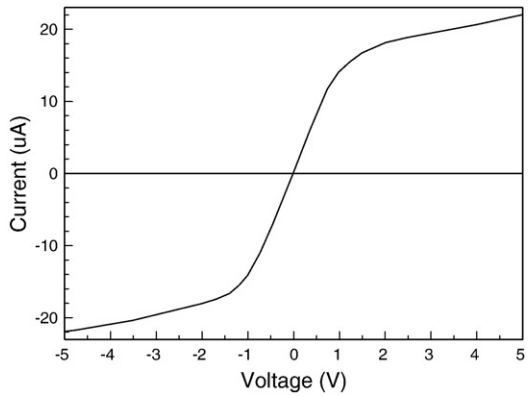

Fig. 3. Current vs. voltage for a single wall nanotube, after Yao [2].

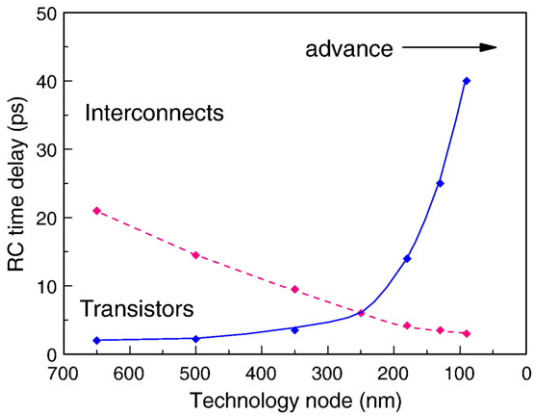

Fig. 4. Time delays in integrated circuits as a function of technology node.

Thus, if MWNTs are used, it is essential to use small diameter MWNTs and to maximise their density. The inter-wall spacing is roughly constant, and similar to the c-axis spacing of graphite, 3.38 Å. For SWNTs, the minimum diameter is 4 Å, but such nanotubes have high free energy and are only made by template growth. The realistic minimum diameter is more like 8 Å. Calculations show that a SWNT areal density of order 10^{14} cm^{-2} are required for interconnect applications. This will be found to be a very high requirement, compared to the state of the art.

Due to the one-dimensional nature of the conductance, it is useful to compare the resistance of CNT interconnects with that of copper, as a function of their length [6] as in Fig. 7. This plot has been calculated for a density of 10^{14} cm^{-2} so it is optimistic. Fig. 7 emphasises that for short interconnects, Cu has a lower resistance than CNTs. The CNT resistance is constant because the extra length does not increase resistance in the ballistic regime. The CNT resistance begins to increase after 1 μm outside the ballistic regime, and is now lower than that of Cu, provided the CNT density is high enough. We see that this is so, if the density is over 10^{13} cm^{-2}.

There are two approaches to work on CNT interconnects. First are those measuring ultimate performance, which tends to use single nanotubes between two points [7,8]. The second is for in-situ growth by chemical vapour deposition (CVD)[9–18], first with 'blanket' films and then in Via holes. Note that it is uneconomic to grow bulk nanotubes, sort them, and then expect to place them in holes. This is not a credible manufacturing process.

Existing work on CNT interconnects has been carried out by Kreupl et al [11–14], and more recently by Awano et al [15–18]. The interconnects grown by both groups are MWNTs. Awano et al [17] have attempted to increase the nanotube density, but are still at about 10^{11} to 10^{12} cm^{-2}. Recently this group [18] used chemical mechanical

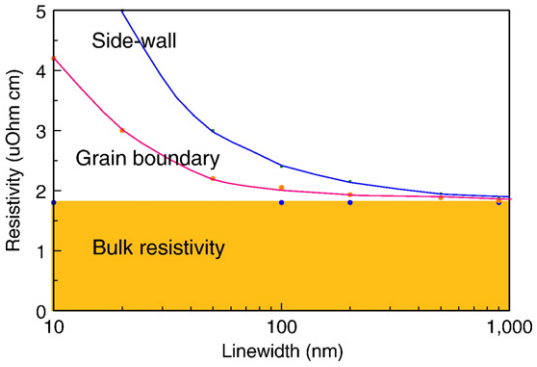

Fig. 5. Copper resistivity vs. interconnect's line-width.

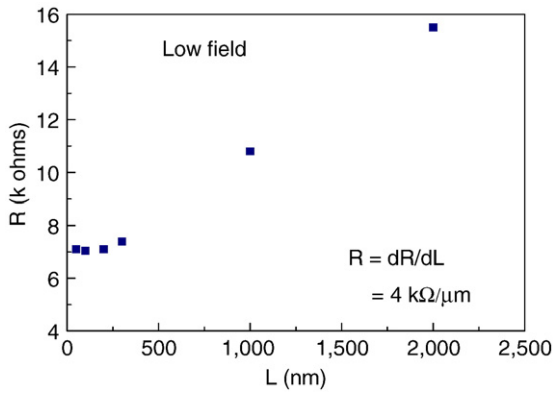

Fig. 6. Resistance vs. nanotube length in low voltage regime, from [2].

polishing to cut the top off the MWNTs to make electrical contact with the inner walls and thus lower the resistance.

Interconnects are 'back end of line' (BEOL) components in integrated circuits, in which the process temperature cannot exceed 400 °C, otherwise there is damage to the inter-metal dielectric. Therefore, the production requires five aspects to be considered,

1. areal density
2. growth temperature
3. fraction of metallic nanotubes
4. growth on conducting metallic surfaces
5. electrical quality

The highest density of nanotubes is found in vertically aligned arrays, mats or forests. Various groups have been able to grow vertical arrays of MWNTs [19–24] and SWNTs [25–42]. Many cases involve the use of an Fe catalyst on a Al_2O_3 support [21,29–36]. Some others use a mixed Co–Mo catalyst on a SiO_2 or Al_2O_3 support [25,38]. The vertical alignment arises from the high density, and is an indication that the density is above about 2.10^{11} cm^{-2}. The work on high vertical arrays is often directed at achieving the highest mats. This is not the case for interconnects, we are interested in achieving the largest areal density. The combination of factors 1, 2 and 4 above is likely to prove quite difficult.

The temperature limits to growth need special attention. The growth process is thermally activated, so at first sight it is expected to be difficult to grow at the low temperatures needed. In practice, the growth process (for nanotubes on surfaces) consists of three steps [42–44](Fig. 8); first the catalyst is deposited as a thin film, second the film is annealed to convert it into a series of catalytically active nanoparticles, and third the nanotubes are grown from the catalyst particles. In CVD, each particle forms a separate nanotube, of about the same diameter.

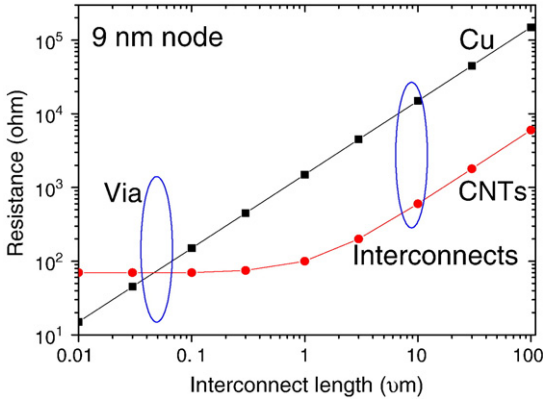

Fig. 7. Calculated resistance vs. length for copper and nanotube interconnects.

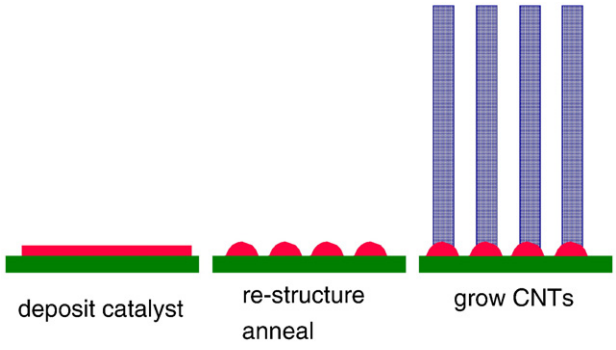

Fig. 8. Schematic of the three steps to nanotube growth, on surfaces.

The re-structuring of the catalyst into nanoparticles occurs in the solid phase by creep [45]. This is thermally activated and easily occurs below the catalyst melting temperature. It is driven by surface energy minimisation. The contact angle of the droplet on a surface is given in terms of interface energies by Young's equation. Forming the nanoparticles occurs by de-wetting and requires a finite contact angle to the support. The re-structuring process is often the rate-limiting step, not the growth itself. The re-structuring step has been observed by in-situ microscopy [45]. The re-structuring temperature can be lowered, if it is carried out prior to exposure to the hydrocarbon growth gas in either a vacuum or in a reducing atmosphere [43]. The ambient gas adsorbs on the catalyst surface and this changes its surface energy, and promotes de-wetting. Often the catalyst becomes oxidised during sample transfer to the growth chamber. It is necessary

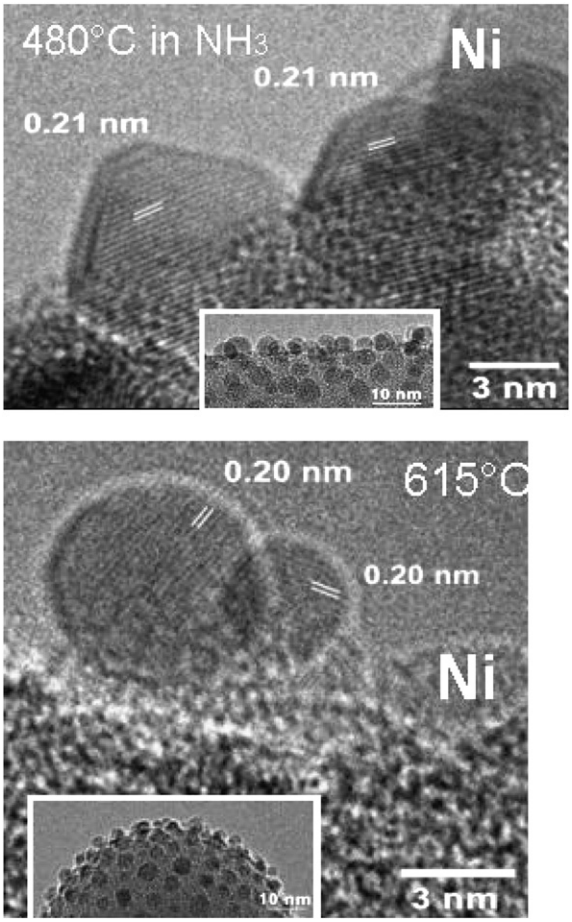

Fig. 9. In-situ TEM images of Ni catalytic nanoparticles after re-structuring in an ammonia atmosphere.

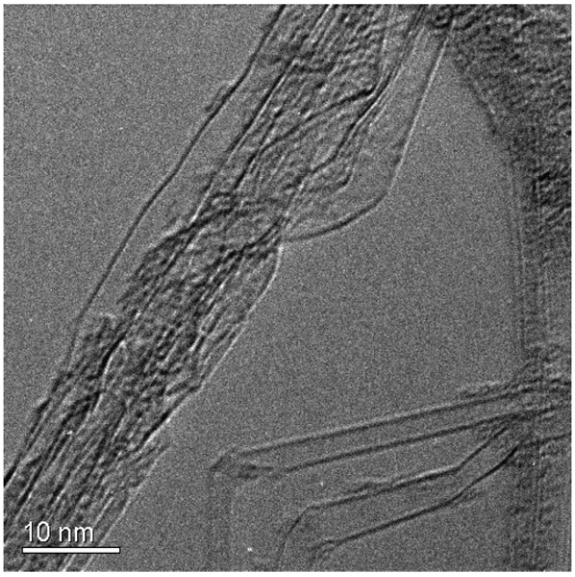

Fig. 10. TEM image of nanotubes, from ref [47].

to reduce the oxide. Depending on the metal, molecular hydrogen may not reduce the oxide; ammonia is more effective. An example is shown in Fig. 9 for Ni in low pressure ammonia atmosphere. After the re-structuring, the growth occurs by turning on the growth gas. Using this method Cantoro et al [42] were able to achieve growth of SWNTs at temperatures as low as 400 °C.

It is also found that a mild plasma is most effective in converting the catalyst into small nanoparticles, especially as the maximum density of particles are needed for high density arrays. Cantoro et al [46] recently found this for MWNTs, following Hofmann et al [43]. Note, however, that strong plasma assistance during growth can be a disadvantage as it disorders the nanotube walls. Only remote plasmas should be used for interconnect applications.

Two particular catalyst-support combinations are found to give high density mats, Fe on Al_2O_3 and Mo–Co catalyst on silica. On the other hand, Fe on SiO_2 support is less effective. On the other hand the Mo–Co combination works because the Mo oxidises and separates the Co as a metal on its surface, where it de-wets into active nanoparticles [39].

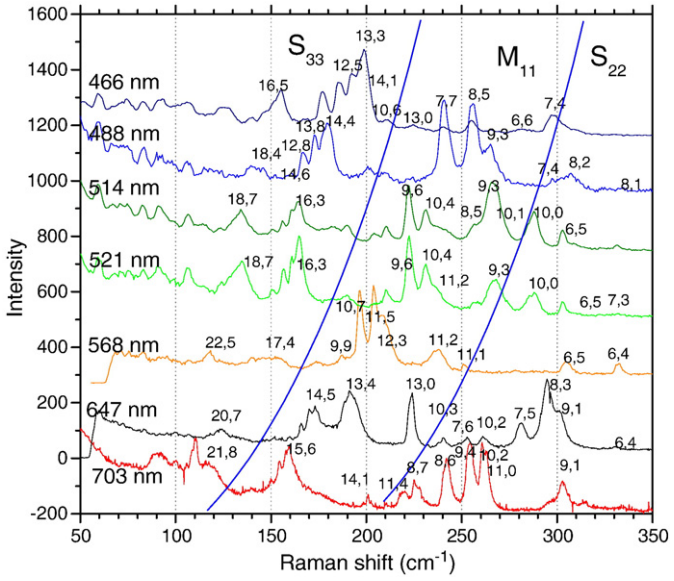

Fig. 11. Radial Breathing Mode assignments of nanotube mat [47].

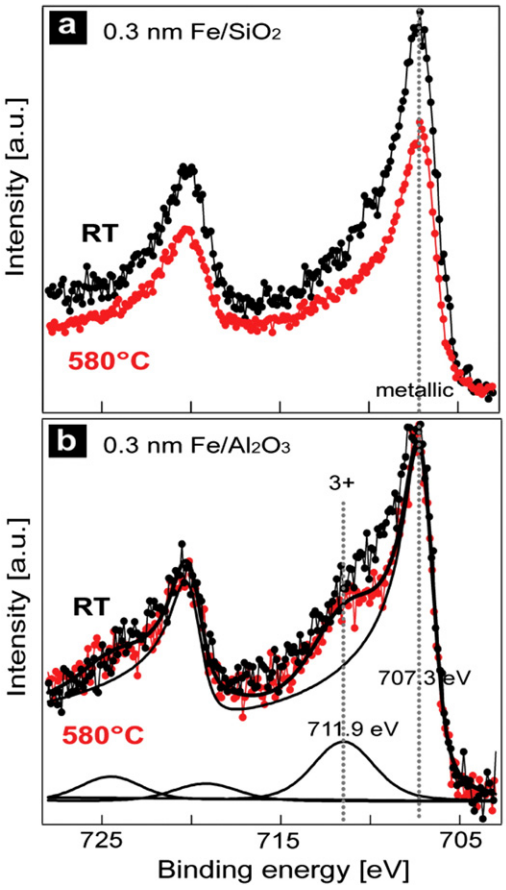

Fig. 12. In-situ photoemission spectra of Fe 2p edges for Fe on SiO_2 and Fe on Al_2O_3 [57].

We grew high density SWNT mats using the Fe–Al_2O_3 combination. First a 20 nm layer of Al is deposited, which oxidises into Al_2O_3. Then a 0.5–1 nm layer of Fe is sputtered, and then another 0.5 nm layer of Al is deposited. The catalyst is heated up to growth temperature of 650 °C in hydrogen. A remote microwave plasma is ignited and growth is carried out in a 10:1 mixture of H_2 and CH_4 at a pressure of 15 mTorr.

The nanotubes formed by the Fe–Al_2O_3 combination were fully characterised by high resolution transmission electron microscopy (TEM) and multi-wavelength Raman. Fig. 10 shows a TEM image of the nanotube mat. Each nanotube type is defined by its integer chiral indices *n*, *m*. Fig. 11 shows the Raman spectra in the region of the radial breathing modes (RBMs). The Raman is measured on the mat, as grown, without dispersing them in a surfactant. The RBM vibrational frequencies vary inversely as the nanotube diameters. They are only excited when the laser energy resonates with an optical transition. The transition energies vary inversely with the nanotube diameter in the so-called Kataura plot. This allows us to assign each RBM mode peak to a SWNT of particular chiral index based on its wavenumber and on its resonant energy [47]. The assignments were

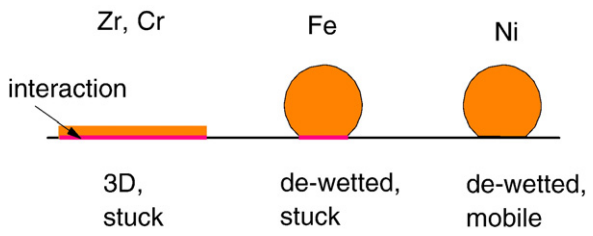

Fig. 13. Schematic of behaviour of various metal nanoparticles on oxide support.

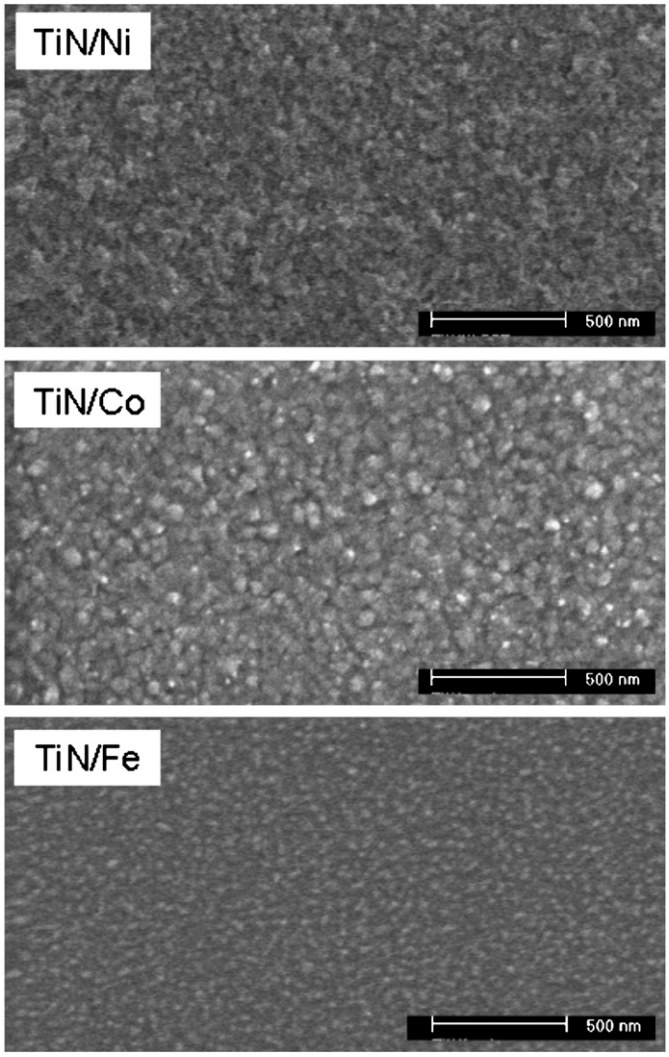

Fig. 14. SEM image of Ni, Co and Fe film on TiN surface after plasma treatment.

carried out for our samples, as they extend over a wider diameter range than previous assignments [48–52]. We find that the RBM wavenumber ω (cm^{-1}) varies with the nanotube diameter d (nm) as

$$\omega = C_1 / d + C_2$$

with $C_1 = 220.4$ and $C_2 = 7.4$. This compares with evaluations of $C_1 = 214.4$ and $C_2 = 18.7$ found by Telg et al [48] and $C_1 = 217.8$ and $C_2 = 15.7$ by Fantini et al [50,51] for HiPCo tubes dispersed in surfactant.

The assignments are shown in Fig. 11. The RBMs divide into certain regions, those corresponding to semiconducting (S) tubes and those corresponding to metallic (M) tubes. We see that there are a large fraction of metallic tubes. The peak heights cannot be directly converted into abundances. We used the matrix elements of Luo et al to [53] derive approximate abundances. We estimate that approximately 1/3 of the tubes in our samples are metallic. This is the same as in a uniform distribution. It is consistent with the wide distribution found by Hata et al [29,32] in their samples also grown from a similar Fe on Al_2O_3 catalyst system.

This conclusion is important as in many cases, lowering the growth temperature or developing particular selective catalysts leads to the preferential growth of more semiconducting tubes. This was found by Maruyama et al [25] for the Co–Mo system, Bachilo et al [54], Dai et al [55], and also recently by Qu et al [56] for the Fe –Al_2O_3 system. This latter result shows that the catalyst and the growth conditions are critical.

The reason for the different behaviour of Fe on Al_2O_3 and SiO_2 was studied by a combination of in-situ photoemission and AFM measurements [57,58]. Fig. 12 shows the core levels of a nominal 0.3 nm thick Fe catalyst layer on SiO_2 and on Al_2O_3 supports during growth. This shows that on SiO_2, the Fe is in its metallic state, whereas there is a slight peak due to Fe^{3+} oxide, due to a thin interfacial Fe oxide in contact with the Al_2O_3. The oxide helps to anchor the metallic Fe nanoparticle to the support oxide, and stop it from sintering into a larger particle. The AFM measurements [57] then showed that the Fe nanoparticles had a much narrower diameter distribution on Al_2O_3 than on SiO_2. An analysis of the resulting nanotubes in TEM found a narrower diameter distribution. This indicates that the Fe particles were less prone to sintering on Al_2O_3. This effect is modelled schematically that Fe on Al_2O_3 has a weak enough interaction to allow the de-wetting, but a strong enough interaction to inhibit the surface diffusion of the Fe balls, and the sintering (Fig. 13).

Despite the excellent results obtained by us on the Fe–Al_2O_3 system, it is clear that it is not possible to use this combination for interconnects, as Al_2O_3 is an insulator. Its results are only guidance. Nanotubes must be grown on conducting substrates for electrical contact. We have now carried out preliminary work for Fe catalysts on Ta and TiN layers. These two metals are widely used in microelectronics as diffusion barriers. Ta was previously used as a barrier layer by Horibe et al [16]. Metals are generally less favourable as catalyst supports because their higher surface energy discourages the catalyst de-wetting. However, Ta is one of the better metals [59,60] and is used by Awano et al [17]. We have found that de-wetting can be induced by a mild plasma treatment, followed by growth in normal thermal CVD conditions. Fig. 14 shows an SEM image of 0.5 nm Ni, Co or Fe on TiN after treatment. Fig. 15 shows a SEM image of a resulting nanotube mat grown a 600 °C. These nanotubes are so far only MWNTs.

2. Summary

The requirements for nanotubes to be used as interconnects in future integrated circuits are described. The conditions for the growth of the nanotubes by chemical vapour deposition are defined in terms of low temperature, high density, metallic quality and growth on metallic substrates. Some examples of nanotubes grown by CVD are given, and their characterisation using TEM and Raman is described. Preliminary work on growing nanotubes on metallic substrates is described.

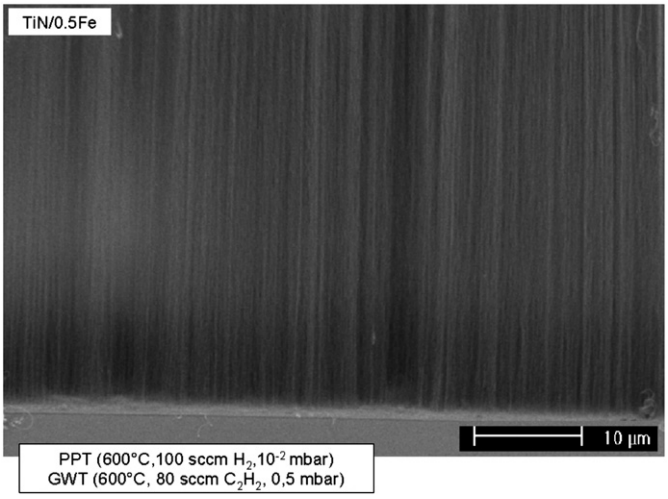

Fig. 15. Side view SEM of nanotube mat grown from 0.5 nm Fe catalyst on TiN.

References

[1] ITRS roadmap www.itrs.net.
[2] Z. Yao, C. L Kane, C. Dekker, Phys. Rev. Lett. 84 (2000) 2941.
[3] J. Kong, E. Yenilmez, T.W. Tombler, W. Kim, H. Dai, R.B. Laughlin, L. Liu, C.S. Jayanthi, S.Y. Wu, Phys. Rev. Lett. 87 (2001) 106801.
[4] C.V. Thompson, presented at Materials Research Society meeting (spring 2008); 46th IEEE Int Reliability Physics Symposium, 2008, p. 368.
[5] J. Y Park, S. Rosenblatt, Y. Yaish, V. Sazonova, H. Ustunel, S. Braig, T. A Arias, P. W Bronner, P. L McEuen, Nano Lett. 4 (2004) 517.
[6] J. Robertson, G. Zhong, H. Telg, C. Thomsen, J. M Warner, G. A D Briggs, U. Detlaff, S. Roth, J. Dijon, Phys. Status Solidi, B 245 (2008) 2303.
[7] G. F Close, S. Yasuda, B. Paul, S. Fujita, H. S P Wong, Nano Lett. 8 (2008) 706.
[8] A. Naeemi, J. D Meindl, IEEE Trans. Ed. 54 (2007) 26.
[9] B.Q. Wei, R. Vajtai, P.M. Ajayan, Appl. Phys. Lett. 79 (2001) 1172.
[10] J. Li, M. Meyyappan, Appl. Phys. Lett. 82 (2003) 2491.
[11] F. Kreupl, A.P. Graham, G.S. Duesberg, W. Steinhoegl, M. Liebau, E. Unger, W. Honlein, Microelectron. Eng. 64 (2002) 339.
[12] F. Kreupl, A.P. Graham, M. Liebau, G.S. Duesberg, R. Seidel, E. Unger, Electron Dev. Meeting, IEDM Tech Digest, 2004, p. 683.
[13] A.P. Graham, G.S. Duesberg, R. Seidel, M. Liebau, E. Unger, F. Kreupl, W. Honlein, Diamond Relat. Matter. 13 (2004) 1296;
Appl. Phys., A 80 (2005) 1141.
[14] G.S. Duesberg, A.P. Graham, F. Kreupl, M. Liebau, R. Seidel, E. Unger, W. Hoenlein, Diamond Rel. Mater. 13 (2004) 354.
[15] M. Nihei, A. Kawabata, Y. Awano, Jpn. J. Appl. Phys. 42 (2003) L721;
M. Nihei, M. Horibe, A. Kawabata, Y. Awano, Jpn. J. Appl. Phys. 43 (2004) 1856;
M. Nihei, A. Kawabata, D. Kondon, M. Horibe, S. Sato, Y. Awano, Jpn. J. Appl. Phys. 44 (2004) 1626;
D. Kondo, S. Sato, Y. Awano, Chem. Phys. Lett. 422 (2006) 481.
[16] M. Horibe, M. Nihei, D. Kondo, A. Kawabata, Y. Awano, Jpn. J. Appl. Phys. 44 (2005) 5309.
[17] Y. Awano, S. Sato, D. Kondo, M. Neihi, Phys. Status Solidi, A 203 (2006) 3611.
[18] D. Yokoyama, T. Iwasaki, K. Ishimaru, S. Sato, T. Hyakushima, M. Nihei, Y. Awano, H. Kawarada, Jpn. J. Appl. Phys. 47 (2008) 1985.
[19] S. S Fan, M. G Chapline, N. R Franklin, T. W Tombler, A. M Cassell, H. Dai, Science 283 (1999) 512.
[20] X. Li, A. Cao, Y. J Jung, R. Vajtai, P. M Ajayan, Nano Lett. 5 (2005) 1997.
[21] A.J. Hart, A.H. Slocum, J. Phys. Chem., B 110 (2006) 8250;
L. Delzeit, C.V. Nguyen, B. Chen, A. Cassell, J. Han, M. Meyyappan, J. Phys. Chem., B 106 (2002) 5629.
[22] M. Pinault, V. Pichot, H. Khodja, P. Launois, C. Reynaud, M. M L, Hermitage, Nano Lett. 5 (2005) 2394.
[23] G. Eres, A. A Puretzky, D. B Geohegan, H. Cui, Appl. Phys. Lett. 84 (2004) 1759.
[24] A.A. Puretzky, D.B. Geohegan, S. Jesse, I.N. Ivanov, G. Eres, Appl. Phys., A 81 (2005) 223.
[25] Y. Miyauchi, S. Chiashi, Y. Murakami, Y. Hayashida, S. Maruyama, Chem. Phys. Lett. 387 (2004) 198.
[26] M. Hu, Y. Murakami, M. Ogura, S. Maruyama, T. Okubo, J. Catal. 225 (2004) 230.
[27] S. Noda, K. Hasegawa, H. Sugime, K. Kazunori, Z. Zhang, S. Maruyama, Y. Yamaguchi, Jpn. J. Appl. Phys. 46 (2007) L399.
[28] R. Xiang, Z. Yang, Q. Zhang, G. Luo, W. Qian, F. Wei, M. Kadowaki, E. Einarsson, S. Maruyama, J. Phys. Chem., C 112 (2008) 4892.
[29] K. Hata, D. N Futuba, K. Mizuno, T. Namai, M. Yumura, S. Iijima, Science 306 (2004) 1362.
[30] D. N Futaba, K. Hata, T. Yamada, K. Yamada, M. Yumura, S. Iijima, Phys. Rev. Lett. 95 (2005) 056104.
[31] D. N Futaba, K. Hata, T. Namai, T. Yamada, K. Mizuno, Y. Hayamizu, M. Yumura, S. Iijima, J. Phys. Chem., B 110 (2006) 8035.
[32] T. Yamada, T. Namai, K. Hata, D. N Futaba, K. Mizuno, J. Fan, M. Yudasaka, M. Yumura, S. Iijima, Nat. Nanotechnol. 1 (2007) 131.
[33] G. Zhong, T. Iwasaki, K. Honda, Y. Ohdomari, H. Kawarada, Jpn. J. Appl. Phys. 44 (2004) 1558.
[34] T. Iwasaki, G. F Zhong, T. Aikawa, T. Yoshida, H. Kawarada, J. Phys. Chem. B 109 (2005) 19556.
[35] G. Zhong, T. Iwasaki, H. Kawarada, Carbon 44 (2006) 2009.
[36] G. Zhong, T. Iwasaki, J. Robertson, H. Kawarada, J. Phys. Chem., B 111 (2007) 1907.
[37] Y. Q Xu, R. E Smalley, R. H Hauge, J. Am. Chem. Soc. 128 (2006) 6560.
[38] L. Zhang, Y.Q. Tan, D.E. Resasco, Chem. Phys. Lett. 422 (2006) 198.
[39] J. E Herrera, L. Balzano, A. Brogna, D. E Resasco, J. Catal. 204 (2001) 129.
[40] L. B Zhu, Y. H Xiu, D. W Hess, C. P Wong, J. Phys. Chem., B 110 (2006) 5445.
[41] H. Ohno, D. Takagi, K. Yamada, S. Chiashi, A. Tokura, Y. Homma, Jpn. J. Appl. Phys. 47 (2008) 1956.
[42] M. Cantoro, S. Hofmann, S. Pisana, V. Scardaci, A. Parvez, C. Ducati, A.C. Ferrari, A.M. Blackburn, K.Y. Wang, J. Robertson, Nano Lett. 6 (2006) 1107.
[43] S. Hofmann, M. Cantoro, B. Kleinsorge, C. Casiraghi, A. Parvez, J. Robertson, C. Ducati, J. Appl. Phys. 98 (2005) 034308.
[44] J. Robertson, Mater. Today 10 (2007) 38.
[45] S. Hofmann, R. Sharma, C. Ducati, G. Du, C. Mattevi, C. Cepek, M. Cantoro, S. Pisana, A. Parvez, F. Cervantes-Sodi, A.C. Ferrari, R.E. Dunin-Borkowski, J. Robertson, Nano Lett. 7 (2007) 602.
[46] M. Cantoro, S. Hofmann, C.T. Wirth, J. Robertson, J. Appl. Phys. (in press).
[47] J. Robertson, G. Zhong, H. Telg, C. Thomsen, J. H Warner, G. A D Briggs, U. Detlaff, S. Roth, Appl. Phys. Lett. 93 (2008) 163111.
[48] H. Telg, J. Maultzsch, S. Reich, F. Heinrich, C. Thomsen, Phys. Rev. Lett. 93 (2004) 177401.
[49] J. Maultzsch, H. Telg, S. Reich, C. Thomsen, Phys. Rev., B 72 (2005) 205438.
[50] C. Fantini, A. Jorio, M. Souza, M. S Strano, M. S Dresselhaus, M. A Pimenta, Phys. Rev. Lett. 93 (2004) 147406.
[51] P. T Araujo, S. K Doorn, S. Kilina, S. Tretiak, E. Einarsson, A. Jorio, Phys. Rev. Lett. 98 (2007) 067401.
[52] P. T Araujo, I. O Marcel, P. B C Pesce, M. A Pimento, A. Jorio, Phys. Rev., B 77 (2008) 241403.
[53] Z. Luo, F. Papadimmitrakopoulos, S. K Doorn, Appl. Phys. Lett. 88 (2006) 073110.
[54] S. M Bachilo, L. Balzano, J. E Herrera, F. Pompeo, D. E Resasco, R. B Weisman, J. Am. Chem. Soc. 125 (2003) 11186.
[55] Y. Li, D. Mann, M. Rolandi, W. Kim, A. Ural, S. Huang, A. Javey, D. Wang, E. Yenilmez, Q. Wang, J. F Gibbons, Y. Nishi, H. J Dai, Nano Lett. 4 (2004) 317.
[56] L. Qu, F. Du, L. Dai, Nano Lett. 8 (2008) 2682.
[57] C. Mattevi, C. T Wirth, S. Hofmann, R. Blume, M. Cantoro, C. Ducati, C. Cepek, A. Knop-Gericke, A. Goldoni, R. Schlogl, J. Robertson, J. Phys. Chem., C 112 (2008) 12207.
[58] S. Hofmann, R. Blume, C.T. Wirth, M. Cantoro, R. Sharma, C. Ducati, M. Havecker, S. Zafeiratos, P. Schnoerch, A. Oestereich, D. Teschner, M. Albrecht, A.S. Knop-Gericke, R. Schlgol, J. Robertson, J. Phys. Chem. C 113 (2009) 1648.
[59] Y. Wang, Z. Luo, B. Li, P. S Ho, Z. Yao, E. N Bryan, R. J Nemanich, J. Appl. Phys. 101 (2007) 124310.
[60] A. L Giermann, C. V Thompson, Appl. Phys. Lett. 86 (2005) 121903.